Enhanced bed load sediment transport by unsteady flows in a degrading channel

Zhijing Li, Honglu Qian, Zhixian Cao, Huaihan Liu, Gareth Pender, Penghui Hu

www.elsevier.com/locate/ijsrc

PII: S1001-6279(16)30072-5
DOI: https://doi.org/10.1016/j.ijsrc.2018.03.002
Reference: IJSRC167

To appear in: *International Journal of Sediment Research*

Received date: 1 November 2016
Revised date: 26 January 2018
Accepted date: 6 March 2018

Cite this article as: Zhijing Li, Honglu Qian, Zhixian Cao, Huaihan Liu, Gareth Pender and Penghui Hu, Enhanced bed load sediment transport by unsteady flows in a degrading channel, *International Journal of Sediment Research,* https://doi.org/10.1016/j.ijsrc.2018.03.002

Enhanced bed load sediment transport by unsteady flows in a degrading channel

Zhijing Li [a, b], Honglu Qian [a], Zhixian Cao [a,*], Huaihan Liu [c], Gareth Pender [d], Penghui Hu [a]

[a] State Key Laboratory of Water Resources and Hydropower Engineering Science, Wuhan University, Wuhan 430072, China

[b] Changjiang River Scientific Research Institute, Wuhan 430015, China

[c] Yangtze River Waterway Bureau, Wuhan 430010, China

[d] School of Energy, Geoscience, Infrastructure and Society, Heriot-Watt University, Edinburgh EH14 4AS, UK

* Corresponding author: Professor Zhixian Cao, Email: *zxcao@whu.edu.cn*

ABSTRACT

Laboratory flume experiments were done to investigate bed load sediment transport by both steady and unsteady flows in a degrading channel. The bed, respectively composed of uniform sand, uniform gravel, or sand-gravel mixtures, always undergoes bulk degradation. It is found that both uniform and non-uniform bed load transport is enhanced greatly by unsteady flows as compared to their volume-equivalent steady flows. This enhancement effect is evaluated by means of an enhancement factor, which is shown to be larger with a coarser bed and lower discharges. Also, the fractional transport rates of gravel and sand in non-uniform sand-gravel mixtures are compared with their uniform counterparts under both steady and unsteady flows. The sand is found to be able to greatly promote the transport of gravel, whilst the gravel considerably hinders the transport of sand. Particularly, the promoting and hindering impacts

are more pronounced at lower discharges and tend to be weakened by flow unsteadiness.

Keywords: Bed load; Gravel; Sand; Unsteady flow; Enhancement effect

1. Introduction

To date bed load sediment transport has been widely studied in idealized cases with steady and uniform flow conditions, which evokes the development of a plethora of formulas for bed load transport (e.g., Einstein, 1950; Engelund & Hansen, 1967;Meyer-Peter&Müller, 1948; Parker, 1990; Wilcock & Crowe, 2003; Wu et al., 2000). However, fluvial flows in natural rivers are typically characterized by unsteady flow hydrographs, such as flood waves and the release flow hydrographs from reservoirs. Another notable feature of natural rivers is the non-uniform composition of both the sediment being transported and that in the riverbeds(Bagnold, 1977).The study of unsteady flow-driven bed load transport, especially with non-uniform sediment composition, is important for both theoretical research and engineering practice.

Although advanced mathematical models for bed load transport under unsteady flows are available now (e.g., Capart& Young, 1998; Hu et al., 2014; Qian et al., 2015; Wu, 2004), the development of these models is inevitably limited by the lack of reliable measured data, which should be collected by field observations or laboratory experiments. It is inspiring that the last several decades have witnessed a few field observations of bed load sediment transport under unsteady floods. For example, Kuhnle (1992) measured bed load transport on two small streams and found that bed load transport rates were greater during rising stages than during falling stages at high flows while the opposite case was observed for low flows. Laronne and Reid (1993) and Reid and Laronne (1995) observed very high rates of bed load sediment transport in an ephemeral desert river - Nahal Yatir, which shows as much as 400 times the efficiency in transporting materials compared to its perennial counterpart - Oak Creek - in humid zones. Other field observations focused on the influence of sand on gravel transport (e.g., Ferguson et al., 1989), the bed load pulses (e.g., Cudden & Hoey, 2003), and the measurement efficiency of bed load transport (e.g., Habersack et al., 2001). These

observations and findings greatly improve the understanding of bed load sediment transport by unsteady flows. But unfortunately, due to real-time measurement difficulties, the available field data are far from sufficient for a full understanding of the hydro-morphodynamics or for testing mathematical models, as they usually concern only one or two of flow stage, bed deformation, sediment transport rate, and bed sediment composition at a single cross-section.

Comparatively, laboratory experiments can be done under controlled conditions, and, thus, there have been an increasing number of experimental investigations of unsteady flow-driven bed load sediment transport. To date, however, most of previous experiments are restricted to cases of uniform sediment (Bombar et al., 2011; Graf & Qu, 2004; Graf & Suszka, 1985; Griffiths & Sutherland, 1977; Lee et al., 2004; Phillips & Sutherland, 1990; Song & Graf, 1997). It has been demonstrated that the bed load transport rates under unsteady flows are larger than those in equivalent steady flows (Graf & Suszka, 1985; Lee et al., 2004). Also, time lags were observed to exist between peaks of flow discharge and bed load sediment transport (Bombar et al., 2011; Graf & Qu, 2004; Lee et al., 2004; Phillips & Sutherland, 1990). The bed load yields during the rising and falling periods of the flow hydrographs are different (Bombar et al., 2011; Lee et al., 2004), though there have been no consistent conclusions (i.e., greater during the rising period or falling period) and the mechanism behind these results is still unclear.

Recent years have witnessed experimental studies on non-uniform bed load transport under unsteady flows. One of the emphases is focused on sediment sorting. For example, Yen and Lee (1995) did experiments with five triangular inflow hydrographs to investigate bed deformation and sediment sorting in a channel bend. Hassan et al. (2006) and Parker et al. (2007) focused on the effect of unsteady hydrographs on the formation and degree of bed surface armouring, while Lunt and Bridge (2007) studied the formation and sorting of gravel strata as related to bed forms. Mao (2012) and Wang et al.(2015) gave insights into the

characteristics of both bed load sediment transport and sediment sorting under unsteady flow hydrographs. Unfortunately, to date, the effect of flow unsteadiness on non-uniform bed load sediment transportremains fragmented and incompletely understood, especially as compared to its counterpart for equivalent steady flows. Wang et al. (2015) did a series of flume experiments without quantitative evaluation. Also, the interaction between various grain size fractions(e.g., influence of sand on gravel transport or that of gravel on sand transport), which was revealed for steady flows (e.g., Kuhnle, 1993; Li et al., 2016; Wilcock, 1998; Wilcock et al., 2001),was missing for unsteady flows. Equally importantly, there is still a lack of a dataset including all of flow stage, bed deformation, sediment transport rate, and bed sediment composition to support the development of mathematical models.

The current study aims to generate a new observed dataset of flume experiments to enhance the understanding of bed load transport by unsteady flows, which can also be used to validate and test mathematical river models. Flume experiments were done using both uniform and non-uniform sediment beds under a range of steady and unsteady inflows. Well-sorted gravel and sand were used to compose four kinds of sediment beds, with sand contents of 0, 47, 78 and 100%. Each sediment bed was subjected to four different inflows, including two unsteady flow hydrographs and two volume-equivalent steady flow hydrographs. Thus, a total of 16 runs of clear-water scour experiments were done. For each run, detailed data on flow stage, bed elevation, fractional bed load transport rates, and bed surface composition were collected. For the first time the effect of flow unsteadiness on bed load sediment transport is studied quantitatively by introducing an enhancement factor. Also, similar to the authors' previous work in Li et al. (2016) for steady flows, the impact of the sand/gravel content in sediment beds on the gravel/sand transport (i.e. the promoting/hindering impact) is evaluated for unsteady flows.

2. Experimental setup and method

The experimental material (i.e. sediment samples), flume set-up, and methods for hydraulic and bed surface composition measurements are essentially similar to those for the experiments on bed load transport in steady flows (Li et al., 2016). Hence these are only briefly described in the following subsections.

2.1. Experimental material - sediment

Four sediment samples used in Li et al.(2016), i.e. samples A, B, C, and D (Table 1 and Fig. 1), were used to compose sediment beds in the current experiments. Sample A, 100% gravel, utilized spherical ceramic balls with a diameter ranging from 2.0 mm to 4.0 mm. Sample B, 100% sand, varying between 0.1 mm and 2.0 mm in diameter, was obtained by sieving natural sand. Samples C and D were made by mixing Samples A and B according to the mass ratios of 1:1 and 1:4 (i.e. the volumetric proportion of sand was 47% and 78%), respectively. Particularly, because of the color difference between the white gravel and yellow sand, a grid-by-number method using photographs of the bed can be used to measure the bed surface composition conveniently (Adams, 1979; Wilcock & McArdell, 1993).

Table 1. Physical characteristics of bed sediment

Sample	Material	Median size (mm)	Color	Density (kg/m^3)	Porosity
A	100% gravel	3.1	White	2390	0.426
B	100% sand	0.67	Yellow	2650	0.412
C	53% gravel, 47% sand	2.0	/	2513	0.420
D	22% gravel, 78% sand	0.8	/	2593	0.415

The "/" means the color of bed sediment is hard to define due to the mixing of gravel and sand with different colors.

Fig. 1. Size distribution of bed sediment

2.2. Flume set-up and hydraulic measurements

The experiments were done in a 35 m long, 1.2 m wide, and 0.8 m deep flume (Fig. 2). A computer-controlled inverter was attached to the pump system, which was capable of producing controlled and unsteady inflow hydrographs with any desired shape. The channel bed consisted of a 20 m long fixed bed and a 12 m long sediment bed. Both the slopes of the fixed and sediment beds were set to be 0.003. At the downstream end of the sediment bed, there was a rigid sill with the same height as the bed layer to prevent local scour and to avoid backwater effects. Downstream of the channel bed was a V-shaped, 1 m long and full-width sediment trap and an adjustable tailgate (Fig. 2b).

The sediment in the trap was collected every 20 min by operating two valves of the trap (Fig. 2d), without the need to shut the flow off. Specifically, Valve B was initially closed while Valve A is open, thus, the sediment settled in the pipe between Valve A and Valve B (see the left picture in Fig. 2d). At the end of each 20-min period, Valve A was closed while Valve B was open in order to quickly collect the accumulated sediment, as shown in the right picture in Fig. 2d. During this short period of operation, the trapped sediment was placed above Valve A. As soon as the collection was finished, Valve B was closed while Valve A was opened again, and the sediment trapping and collection began for another 20-min period. This time interval (i.e. 20 min), which was determined by a trial-and-error procedure, is appropriate for reducing the sediment transport fluctuations during sampling and also for capturing the variation of the sediment transport rate with flow discharge. The collected sediment was then dried and weighed (also sieved for non-uniform cases), so as to obtain the amount of transported sediment or the sediment transport rate in each 20-min period. Also, the average sediment transport rate during the whole period of each run could be calculated readily.

Apart from the sediment transport, detailed measurements of flow stage and bed topography

were also conducted. As shown in Fig. 2b, the water level at four cross sections ($x = 0$, 4, 8, and 12 m) was monitored by four automatic water-level probes (the flow direction is denoted as the x-axis and the origin of the x-axis is taken at the junction of the fixed and mobile sediment beds). The sampling frequency was set at 2 Hz and the corresponding measurement error was within ±0.5 mm. In addition, two automatic terrain monitors mounted on the sidewalls of the flume were used to track the bed evolution at two cross sections ($x = 2$ and 6 m) every 10 min. The final bed topography was also measured at the end of each run, at cross sections 20 cm apart in the first 4 m reach of the mobile-bed section, and in the remaining reach at cross sections 40 cm apart. For each cross section, the bed elevations were measured at 13 points with a lateral spacing of 10 cm and a measurement error of ±0.6 mm.

Fig. 2. Flume set-up: (a) perspective view; (b) top view; (c) side view; (d) sediment trap (after Li et al., 2016)

2.3. Bed surface composition

In recent years, a grid-by-number method using photographs of the bed has been widely used to determine the bed surface composition (e.g., Mao, 2012; Wang et al., 2015; Wilcock & McArdell, 1993; Wilcock et al., 2001), as it facilitates non-destructive sampling and can be implemented through the flowing water without shutting the flow off. The accuracy of this method has been demonstrated to be equivalent to that of the traditional volume-by-weight method commonly used in bulk sampling and sieve analyses (Kellerhals & Bray, 1971).

Generally, this method is implemented by projecting the photographs of the bed onto a grid, and tallying the grain color (hence sand or gravel) falling on the grid intersections. At the end of each run, ten adjacent photographs with a continuous coverage of the 12 m long sediment

bed were first taken, each covering a bed section 1 m wide and 1.2 m long with the remaining 10 cm on each side of the flume not being photographed. Then for each photograph, 500×600 points were counted to obtain the fractions of gravel and sand. The cross-stream and downstream separations between grid points were 2 mm, and the diagonal separation between grid points was 2.8 mm. This spacing is smaller than the largest sediment size on the bed. Also, the bed surface in a particular section of the channel, i.e. $2.4 < x < 3.6$ m, was photographed at 1 h increments during the experiments to investigate the temporal changes of the bed surface composition.

2.4. Flow hydrographs

Two unsteady and two steady flow hydrographs (Fig. 3) were designed and imposed at the flume inlet for the experiments. As shown in Fig. 3,all the hydrographs have the same duration (7 h) and the same base flow ($q = 0.002$ m^2/s) under which no sediment particles can move or be transported. For comparison, the unsteady hydrographs (U1, U2) are designed to have the same total water volume as for the corresponding steady hydrographs (S1, S2). This constant volume is motivated by the release hydrographs of a reservoir, which have a certain water volume but may vary differently in shape. At the beginning of the experiments for steady flows, the discharge rapidly increases from the base value to a constant level in about 2 min, which is short enough to be neglected compared with the experimental duration (7 h). The two unsteady hydrographs with different peak discharges are characterized by smooth and continuous sinusoidal curves, which are more representative of natural hydrographs than the stepped, triangular or trapezoidal hydrographs (e.g., Bombar et al., 2011; Hassan et al., 2006; Lee et al., 2004; Yen & Lee, 1995).

Fig. 3. Designed flow hydrographs at the flume inlet

2.5. Experimental procedure

Prior to each run, the tailgate was closed and the bed sediment was very slowly filled with water from the downstream end of the flume. After the bed sediment was saturated and there was a thin sheet flow above the bed surface, the tailgate was opened and a small inflow was given and maintained so as to establish an initial condition (i.e. base flow) along the whole flume. The inflow was so weak that no sediment could move or be transported. Then the flow was controlled to the desired hydrograph, and the experiment began. No sediment was fed or recirculated during the experiment, so the sediment bed was subjected to clear-water scouring. This is similar to the bed scouring usually occurring downstream of a dam in a natural river (e.g., the Three Gorges Dam on the Yangtze River, China), where the inflow (i.e. release flow from the reservoir) is nearly clear water. Each run lasted for 7 h, during which there was sufficiently strong bed deformation and obvious changes in bed surface composition.

As summarized in Table 2, a total of 16 runs were done by varying inlet discharge hydrographs (steady or unsteady) as well as bed sediment samples (Samples A, B, C, and D). In Table 2, q is the unit-width flow discharge of the steady flows; q_{peak} is the peak discharge of the unsteady flows; V_{total} is the total water volume of the hydrograph; SI is the suspension index calculated as $SI = \omega/(ku_*)$, where ω is the sediment settling velocity, $\kappa = 0.4$ is the von Karman constant, and u_* is the bed shear velocity. For each run, the peak flow conditions at cross section $x = 12$ m (i.e. flume outlet) are selected to estimate the (minimum) value of the suspension index. As listed in Table 2, the (minimum) suspension indexes in most of the experimental runs are greater than 5.0, which means that the sediment particles are mainly transported as bed load (Chien & Wan, 1999). Although Runs BS2 and

BU2 are the exceptions, the suspension indexes for these runs are very close to 5.0 (i.e. 4.0~5.0).

Table 2. Summary of experiments

Run	Sediment bed	Hydrograph	q (m^2/s)	q_{peak} (m^2/s)	V_{total} (m^3)	SI
AS1	Sample A	S1	0.01	/	302.4	15.1
AS2	Sample A	S2	0.02	/	604.8	13.3
AU1	Sample A	U1	/	0.018	302.4	12.9
AU2	Sample A	U2	/	0.038	604.8	10.2
BS1	Sample B	S1	0.01	/	302.4	6.7
BS2	Sample B	S2	0.02	/	604.8	4.2
BU1	Sample B	U1	/	0.018	302.4	5.3
BU2	Sample B	U2	/	0.038	604.8	4.4
CS1	Sample C	S1	0.01	/	302.4	14.9
CS2	Sample C	S2	0.02	/	604.8	11.0
CU1	Sample C	U1	/	0.018	302.4	10.7
CU2	Sample C	U2	/	0.038	604.8	8.4
DS1	Sample D	S1	0.01	/	302.4	6.3
DS2	Sample D	S2	0.02	/	604.8	5.3
DU1	Sample D	U1	/	0.018	302.4	5.4
DU2	Sample D	U2	/	0.038	604.8	5.0

The "/" indicates no constant or uniform flow discharges for runs with unsteady inflows, and no peak flow discharges for runs with steady inflows.

3. Results

For each run, complete measurements were made, including flow stage, bed elevation, sediment transport rate, and bed surface composition. These data are sufficient to be used to validate and test mathematical river models. Here, some typical results are presented to illustrate the unsteady flow-driven bed load transport processes. Particularly, the effects of flow unsteadiness and non-uniform sediment composition on bed load transport are evaluated by analyzing the collected bed load data for all runs.

3.1. Stage

Figure 4 shows the stage hydrographs at four different cross sections ($x = 0$, 4, 8, and 12 m) for Run DU2.The bed elevation at cross section $x = 0$ m is set to 0 m. It can be seen that the observed stage increases from an initial value to the peak level and then falls gradually, which is consistent with the designed flow hydrograph for Run DU2 (Fig. 3). Further, the stages at the four locations decrease successively except that the stage at the second cross section ($x =$ 4 m) is higher than that at the first cross section ($x = 0$ m) between $t = 120$ min and 300 min due to the formation of a hydraulic jump induced by strong flow strength and bed deformation. Water surface slope can be estimated roughly from the observed stages at the four cross sections along the entire sediment bed. Particularly, the stage hydrographs at $x = 0$ m and $x = 12$ m can be used as inlet and outlet boundary conditions, respectively, for mathematical river modelling. Because a free overfall occurs at the downstream end of the sediment bed with a fixed and unadjustable rigid sill, stage conditions vary according to different inlet discharge hydrographs. The stage measurements for other experimental runs are not presented here for simplicity but can be made available upon request.

Fig. 4. Observed stage hydrographs at different cross sections for Run DU2

3.2. Bed elevation

Figure 5 shows the measured bed elevation for Run DU2. Significant degradation can be noticed from the final bed configuration (Fig. 5a) or bed profile (Fig. 5b), yet the intense scour is mainly confined to the upstream part ($x < 6$ m) of the sediment bed while only a thin sediment sheet is eroded from the downstream bed. In this connection, a similar phenomenon has been observed by Wong and Parker(2006) wherein the bed deformation is restricted to a short distance near the non-capacity feeding point. This confirms that bed load transport can

adapt to its capacity regime very quickly (Cao et al., 2011). In addition, the time variation of the bed elevations at two cross sections ($x = 2.0$ m and $x = 6.0$ m), which were measured every ten min during the experiments, also is shown for calibrating and testing mathematical models (Fig. 5c).

Fig. 5. Bed elevation for Run DU2: (a) final bed topography (with respect to the initial bed elevation); (b) cross section averaged initial and final bed elevations; and (c) time variation of cross section averaged bed elevations at $x = 2.0$ m and $x = 6.0$ m

3.3. Bed load transport rate

Bed load sediment was collected every 20 min by the sediment trap, and all samples were air-dried and weighed (also sieved for non-uniform cases). It can be seen from Fig. 6a that the cumulative weight of bed load sediment (gravel, sand, or both) keeps increasing from initially zero until reaching a constant value. Correspondingly, the bed load transport rate averaged in 20-min intervals grows from zero to a peak value and then falls gradually to zero again (Fig. 6b). This bed load transport process also is in accordance with the flow hydrograph (Fig. 3).

Fig. 6. Bed load transport for Run DU2: (a) total weight; and (b) transport rate averaged in 20-min intervals

3.4. Bed surface composition

For cases of non-uniform bed load transport, the sediment bed was firstly photographed and

then the grid-by-number method was used to obtain bed surface composition. Here, F_i is introduced to represent the volumetric proportion of sand (F_s) or gravel (F_g) on the bed surface. Figure 7 shows the variation of bed surface composition for Run DU2 with unsteady inflow. Longitudinally, the final bed sediment composition does not change obviously within x < 4.8 m as compared to the initial bed, whilst the remaining reach (i.e. x > 4.8 m) exhibits a clear coarsening feature (Fig. 7a). Further, a non-monotonic trend is observed for the time variation of the percentages of gravel and sand within subsection 2.4< x <3.6 m, which increase or decrease alternately during the experiment and are finally close to their initial percentages (Fig. 7b). However, for cases with steady inflows (e.g. Run DS2), the final sediment bed always shows a coarsening feature in the whole reach (Fig. 8a), and the bed within subsection 2.4< x <3.6 m gets coarsened roughly over time (Fig. 8b).The differences of the bed surface composition between runs with steady and unsteady inflows are probably because steady and constant flows promote the development of bed coarsening or armoring, whereas unsteady and peak flows tend to subdue or destroy the coarse surface layer or armor layer(Hassan et al., 2006).

Fig. 7. Bed surface composition for Run DU2: (a) the percentage of gravel on the initial and final bed surfaces; and (b) time variation of the percentages of gravel (F_g) and sand (F_s) on the bed surface within subsection 2.4 < x < 3.6 m

Fig. 8. Bed surface composition for Run DS2: (a) the percentage of gravel on the initial and final bed surfaces; and (b) time variation of the percentages of gravel (F_g) and sand (F_s) on the bed surface within subsection 2.4< x <3.6 m

3.5. Enhanced bed load sediment transport by unsteady flow

For bed load transport, two important issues have raised wide concern in recent years, i.e. the effects of flow unsteadiness (e.g. Graf & Suszka, 1985; Laronne & Reid, 1993; Lee et al., 2004; Wang et al., 2015) and of sediment heterogeneity (e.g., Kuhnle, 1993; Li et al., 2016; Wang et al., 2015; Wilcock et al., 2001) on bed load transport. To further shed light on the two issues, detailed data on bed load transport for all runs are collected and listed in Table 3, where W_{Ti} is the total bed load weight during an entire flood hydrograph for either gravel (W_{Tg}) or sand (W_{Ts}); W_{Ri} is the bed load collected during the rising period of a flood hydrograph for either gravel (W_{Rg}) or sand (W_{Rs}); W_{Fi} is the bed load collected during the falling period of a flood hydrograph for either gravel (W_{Fg}) or sand (W_{Fs}); q_{bi} is the volumetric transport rate per unit width for either gravel (q_{bg}) or sand (q_{bs}), which is averaged over the duration of the experiments (i.e., 7 h); f_i is the initial proportion of sand (f_s) or gravel (f_g) in the sediment bed, and the scaled bed load transport rate q_{bi}/f_i is introduced for either gravel (q_{bg}/f_g) or sand (q_{bs}/f_s) to eliminate the influence of the contents of the gravel and sand in the sediment mixture on their actual transport rates (i.e. q_{bg} and q_{bs}).

Table 3. Collected bed load data for the experimental runs

Run	W_{Ti} (kg)		W_{Ri} (kg)		W_{Fi} (kg)		q_{bi} ($\times 10^{-7}$ m^2/s)		q_{bi}/f_i ($\times 10^{-7}$ m^2/s)	
	W_{Tg}	W_{Ts}	W_{Rg}	W_{Rs}	W_{Fg}	W_{Fs}	q_{bg}	q_{bs}	q_{bg}/f_g	q_{bs}/f_s
AS1	0.3	0.0	/	/	/	/	0.04	0.00	0.04	0.00
AS2	11.4	0.0	/	/	/	/	1.58	0.00	1.58	0.00
AU1	4.5	0.0	3.1	0.0	1.4	0.0	0.63	0.00	0.63	0.00
AU2	114.8	0.0	70.2	0.0	44.6	0.0	15.90	0.00	15.90	0.00
BS1	0.0	81.1	/	/	/	/	0.00	10.10	0.00	10.10
BS2	0.0	271.6	/	/	/	/	0.00	33.90	0.00	33.90
BU1	0.0	168.9	0.0	103.3	0.0	65.6	0.00	21.10	0.00	21.10
BU2	0.0	440.2	0.0	335.1	0.0	105.1	0.00	54.90	0.00	54.90
CS1	11.2	12.6	/	/	/	/	1.55	1.58	2.92	3.36
CS2	78.7	82.8	/	/	/	/	10.80	10.30	20.40	21.90
CU1	29.3	32.5	19.1	20.4	10.2	12.1	4.05	4.06	7.64	8.64
CU2	141.7	169.6	99.4	113.6	42.4	56.0	19.60	21.20	37.00	45.10
DS1	11.3	41.7	/	/	/	/	1.57	5.20	7.14	6.67
DS2	44.2	174.2	/	/	/	/	6.12	21.70	27.80	27.80
DU1	19.4	90.7	11.9	57.5	7.5	33.2	2.68	11.30	12.20	14.50
DU2	74.2	301.0	50.2	216.6	24.0	84.5	9.26	41.70	42.10	53.50

The "/" means no collected data for rising or falling period when it comes to runs with steady inflows, where flow hydrographs are always constant and uniform without rising or falling process.

Figure 9 shows the scaled bed load transport rates (averaged over the whole period of the experiments) for gravel and sand for all the experimental runs. It can be found in Table 3 and Fig. 9 that the total weights of collected bed load or the scaled bed load transport rates under unsteady flow conditions are always higher than those in volume-equivalent steady flows for both cases with uniform and non-uniform sediment beds. That is to say, bed load transport is enhanced by unsteady flows. Particularly, Table 3 indicates that the bed load collected during the rising period of an unsteady flood hydrograph is greater than that in the falling period, as identified by Hassan et al. (2006) and Mao (2012).Nevertheless, the opposite was also observed (e.g., Lee et al., 2004; Yen & Lee, 1995), i.e. the collected bed load is greater during the falling period than the rising period. Kuhnle (1992) claimed that different findings are attributable to different flow strengths, while Bombar et al. (2011) found that different shapes

of hydrographs give rise to different conclusions. Unfortunately, the mechanism is still far from clear and certainly warrants further investigation.

Fig. 9. Scaled bed load transport rates for gravel and sand for all the experimental runs

Similarly, Lee et al. (2004) and Wang et al. (2015) did experiments for both steady and unsteady flows, and found an enhancement effect of unsteady flows on bed load transport. Unfortunately, no appropriate factors were introduced to further evaluate this effect quantitatively. Therefore as a step forward, an enhancement factor, *En*, is introduced here, defined as the ratio of the bed load transport rate (averaged over the whole period of the experiment) in an unsteady flow to that in its equivalent steady flow. Figure 10 shows the variation of the enhancement factor with flow discharge. It can be seen that the enhancement factors are always larger than one, indicating that unsteady flows indeed have an enhancement effect on bed load transport as compared to their equivalent steady flows. Further, the enhancement factors for cases with $q = 0.01$ m^2/s are all larger than those for cases with $q = 0.02$ m^2/s, which means the enhancement effect seems to be more pronounced at a lower discharge. With the same inflow discharge, the enhancement factors for different sediment beds show a trend of Sample A > Sample C > Sample D > Sample B. In essence, the enhancement effect increases with the coarsening of the sediment bed. When the fractional enhancement factors for gravel (En_g) and sand (En_s) are introduced, their variation trends are similar to the bulk enhancement factor, En, i.e. increasing with the adding of coarse gravel in the sediment bed and being greater at a lower discharge (Fig. 11). It is inferred that for a lower steady flow and a coarser bed, the sediment transport is at low rates, and, thus, tends to be enhanced greatly by unsteady flows. On the contrary, the sediment transport rates

are already high with a greater discharge and a finer bed, so the enhancement effect is less pronounced.

Fig. 10. Variation of the enhancement factor with flow discharge

Fig. 11. Variation of fractional enhancement factor with flow discharge

3.6. Promoting/hindering impacts in non-uniform bed load transport by unsteady flows

The promoting and hindering impacts in non-uniform bed load transport have been studied under steady flow conditions in the authors' previous work (Li et al., 2016). The current study aims to explore the promoting and hindering impacts of unsteady flows. As Table 3 indicates, the scaled transport rates of gravel in non-uniform sand-gravel mixtures are generally higher than those in cases of uniform gravel, but in contrast the scaled transport rates of sand in non-uniform cases are lower than those in uniform counterparts. For further study, Figs. 12-15 exhibit the variation of bed load transport rate averaged by every 20-min interval in runs with both steady and unsteady inflows. For steady inflows, it can be found in Fig. 12a that the total bed load transport rates of Runs CS1 and DS1 are within the range of Runs AS1 and BS1, and as the content of sand increases, the total transport rate increases significantly (i.e. Run AS1 < CS1 < DS1 < BS1). Further, Fig. 12b shows that the scaled transport rate of gravel increases with the addition of the sand content (Runs AS1 < CS1 < DS1), while the scaled transport rate of sand in Fig. 12c decreases as the content of gravel increases (Runs CS1 < DS1 < BS1). Obviously, the fractional transport rates of gravel and sand are affected by their contents in

the bed sediment mixture. This is also true for Fig. 13 with a higher steady inflow and Fig. 14 with a lower unsteady inflow. However, the effects of the gravel/sand content are certainly modulated by the strong stochastic nature of the turbulent flow, especially in the case of the high unsteady flow, and inevitably become less pronounced in Fig. 15.

Under unsteady flow hydrographs, the peak sediment transport usually occurs before or after the peak flow with a small time lag (Bombar et al., 2011; Graf & Qu, 2004; Lee et al., 2004; Phillips & Sutherland, 1990; Wang et al., 2015). However, no significant time lag between the occurrence of peak flow and that of the peak sediment transport rate is observed in the current study (Figs. 14 and 15), as pronounced time lags are difficult to produce in the laboratory because the magnitude of flow unsteadiness as well as the averaging time interval to obtain the sediment transport rate may influence the time lags strongly (Graf & Qu, 2004).

The statistical *t*-test is applied here to examine the significance of the difference between every two experimental runs and to further support the foregoing findings. In this regard, two important hypotheses are introduced. The *null hypothesis* is that the scaled bed load transport rates from two selected experimental runs have no significant difference, while the *alternative hypothesis* is that the scaled bed load transport rates from two selected experimental runs have a significant difference.Then *t*-value is calculated by

$$t_v = \bar{p}/s \tag{1}$$

$$\bar{p} = \sum p_k / n \tag{2}$$

$$s = \sqrt{\frac{\sum (p_k - \bar{p})^2}{n(n-1)}} = \sqrt{\frac{\sum {p_k}^2 - (\sum p_k)^2 / n}{n(n-1)}} \tag{3}$$

where t_v is the *t*-value; p_k is the difference of the bed load transport rates at the *k*th time interval between two selected experimental runs; $n = 22$ is the number of samples (i.e. data points) in each run; $\bar{p}$ is the mean value of p_k; and s is the standard deviation. For a significance level, $\alpha = 0.05$, and a degree of freedom, $f = n - 1 = 21$, the threshold *t*-value is

$t_{0.05}(21) = 2.080$, below which the null hypothesis cannot be rejected.

Table 4 lists the *t*-values for scaled bed load transport rates from every two runs in Figs. 12 to 15. It can be found that only three of the 24 *t*-values are below the threshold 2.080,among which the *t*-value for CS2 vs. DS2 in Fig. 13bis just marginally lower than the threshold and in fact the series of data points in Fig. 13b can be visually distinguished. That means only a few data points in Fig. 15c are really close and have no significant difference due to the strong stochastic nature of the turbulent flow, but in most cases the differences between data points are significant. So the trends found, i.e. the scaled transport rate of gravel increases with the addition of sand while the scaled transport rate of sand decreases as the content of gravel increases, are clear and convincing.

Table 4. Summary of *t*-values

Runs	*t*-value	Remark	Runs	*t*-value	Remark
AS1 vs. CS1	8.130	Fig. 12b (gravel)	AS2 vs. CS2	10.379	Fig. 13b (gravel)
AS1 vs. DS1	13.072		AS2 vs. DS2	7.167	
CS1 vs. DS1	15.726		CS2 vs. DS2	2.008	
BS1 vs. CS1	15.443	Fig. 12c (sand)	BS2 vs. CS2	6.434	Fig. 13c (sand)
BS1 vs. DS1	11.595		BS2 vs. DS2	10.719	
CS1 vs. DS1	11.462		CS2 vs. DS2	3.316	
AU1 vs. CU1	3.413	Fig. 14b (gravel)	AU2 vs. CU2	3.246	Fig. 15b (gravel)
AU1 vs. DU1	3.744		AU2 vs. DU2	3.537	
CU1 vs. DU1	3.927		CU2 vs. DU2	3.714	
BU1 vs. CU1	5.102	Fig. 14c (sand)	BU2 vs. CU2	1.861	Fig. 15c (sand)
BU1 vs. DU1	5.837		BU2 vs. DU2	2.365	
CU1 vs. DU1	3.459		CU2 vs. DU2	0.931	

Fig. 12. Variation of (a) total bed load transport rates (gravel plus sand), (b) scaled gravel transport rates, and (c) scaled sand transport rates for Runs AS1, BS1, CS1, and DS1 with steady inflow

Fig. 13. Variation of (a) total bed load transport rates (gravel plus sand), (b) scaled gravel transport rates, and (c) scaled sand transport rates for Runs AS2, BS2, CS2, and DS2 with steady inflow

Fig. 14. Variation of (a) total bed load transport rates (gravel plus sand), (b) scaled gravel transport rates, and (c) scaled sand transport rates for Runs AU1, BU1, CU1, and DU1 with unsteady inflow

Fig. 15. Variation of (a) total bed load transport rates (gravel plus sand),(b) scaled gravel transport rates, and (c) scaled sand transport rates for Runs AU2, BU2, CU2 and DU2 with unsteady inflow

From the foregoing analysis (Figs. 12-15), it is found that with the same inflows, the scaled transport rates of gravel in cases of sand-gravel mixtures are higher than those in cases of uniform gravel, indicating that the sand promotes the transport of gravel. On the other hand, the scaled transport rates of sand in cases of gravel-sand mixture are lower than those in cases of uniform sand, which means that the gravel hinders the transport of sand. Following the authors' previous work in Li et al.(2016), a promoting factor, F_{sg}, and a hindering factor, F_{gs}, are introduced to quantify the effect of the sand on gravel transport and that of the gravel on sand transport, respectively.

$$F_{sg} = \left(\frac{q_{bg}}{f_g} \right) \Big/ \left(\frac{q_{bgug}}{f_{gug}} \right) \tag{4}$$

$$F_{gs} = \left(\frac{q_{bs}}{f_s} \right) \Big/ \left(\frac{q_{bsus}}{f_{sus}} \right) \tag{5}$$

where the subscript ug denotes uniform gravel and us denotes uniform sand. Obviously, the gravel or sand content f_{gug} or f_{sus} is equal to one in uniform cases.

Figure 16 shows the variation of the impact factors with flow for both steady and unsteady flows. Generally, the value of the promoting factor, F_{sg}, is always greater than one, whereas the value of the hindering factor, F_{gs}, is less than one. This demonstrates that compared with bed load transport for a uniform bed, the sand in a non-uniform sand-gravel mixture exerts a promoting effect on the transport of gravel, and in contrast the gravel has a hindering effect on the sand transport. Moreover, the value of F_{sg} for Runs CS1-CS2 (47% sand) is smaller than that of Runs DS1-DS2 (78% sand), indicating that the promoting impact is proportional to the sand content. The value of F_{gs} for Runs CS1-CS2 (53% gravel) is smaller than that of Runs DS1-DS2 (22% gravel), which means that the hindering impact increases with addition of gravel. Also in Fig. 16, the promoting factors, F_{sg}, in cases with $q = 0.01$ m^2/s are always larger than those in cases with $q = 0.02$ m^2/s, whilst the opposite case is observed for the hindering factors, F_{gs}. That is to say, the promoting and hindering impacts become more pronounced at a lower discharge. Physically, non-uniform sediment transport under steady flows is in general dictated by two factors, i.e. flow strength and interaction between sediment particles of different diameters (i.e. gravel and sand in the current study). For high flows, flow strength usually prevails while the interaction between sediment fractions plays a minor role. For low flows, however, the flow strength is comparatively small, and thus, the interaction between sediment fractions (e.g. the promoting and hindering impacts) becomes more

pronounced. For sediment transport under unsteady flows, the shape of flow hydrographs may be another factor, but it is not considered here as the inlet discharge hydrographs are all designed to be sinusoidal curves. So the foregoing explanations (i.e. flow strength vs. interaction between sediment fractions) are also applicable for sediment transport in unsteady flows.

Finally, it can be seen from Fig. 16 that the promoting and hindering impacts seem to be weakened by unsteady flows, as the promoting factors in unsteady flows are smaller than those in equivalent steady flows, while the hindering factors in unsteady cases are larger than those in equivalent steady cases.

Fig. 16. Variation of impact factors with flow

4. Conclusions

A total of 16 experimental runs were done with steady and unsteady inflows and four sediment samples, i.e. uniform 100% gravel, uniform 100% sand, 53% gravel plus 47% sand, and 22% gravel plus 78% sand. A new observed dataset is collected, including the flow stage, bed elevation, sediment transport rate, and bed surface composition, which can be used to underpin the development of mathematical river models. The experimental data reveal that bed load transport rates of both uniform and non-uniform sediments under unsteady flows are generally higher than their counterparts in volume-equivalent steady flows, which clearly characterizes that unsteady flows enhance bed load transport. This enhancement effect is more pronounced on a coarser bed and at a lower discharge. It is also found that under both steady and unsteady flows, the transport of gravel for a sand-gravel mixture is promoted greatly as compared to its counterpart for uniform gravel, whilst the transport of sand in the mixture is

considerably hindered in comparison with that of uniform sand. Promoting and hindering factors are introduced to quantitatively evaluate the promoting and hindering impacts, which are shown to be more significant at a lower discharge and weakened by the flow unsteadiness. This study facilitates enhanced understanding of bed load sediment transport in degrading channels, which are usually subjected to various unsteady hydrographs.

Declaration: *The raw experimental data can be made available upon request to support future investigations in the general context of river dynamics*.

Acknowledgements

The research is funded by National Natural Science Foundation of China(Grant nos. 11172217 and11432015).

Notation

D_g, D_s = sediment diameters of gravel and sand, respectively [mm]

d_{50} = median sediment size [mm];

En = enhancement factor [–];

En_g, En_s = fractional enhancement factors for gravel and sand, respectively [–];

F_g = proportion of gravel on the bed surface [–];

F_{gs} = impact factor representing the effect of gravel on sand [–];

F_s = proportion of sand on the bed surface [–];

F_{sg} = impact factor representing the effect of sand on gravel [–];

f = degree of freedom [–];

f_g = initial proportion of gravel in the sediment bed [–];

f_s = initial proportion of sand in the sediment bed [–];

i = subscript denoting gravel or sand [–];

n =number of data points [–];

p_k =difference of bed load transport rates between two selected experimental runs for the kth time interval [m^2/s];

$\bar{p}$ =mean value of p_k [m^2/s];

q = unit-width flow discharge [m^2/s];

q_b = unit-width volumetric transport rate [m^2/s];

q_{bg} = unit-width volumetric transport rate of gravel [m^2/s];

q_{bs} = unit-width volumetric transport rate of sand [m^2/s];

q_{peak} = unit-width peak flow discharge [m^2/s];

SI = suspension index [–];

s =standard deviation [–];

t = time [s];

t_v = t-value [–];

ug = subscript denoting cases of uniform gravel [–];

us = subscript denoting cases of uniform sand [–];

u_* = bed shear velocity [m/s];

V_{total} = total water volume [m^3];

W_{Fg}, W_{Fs} = weights of gravel and sand, respectively, during the falling period of a flood hydrograph [kg];

W_{Rg}, W_{Rs} = weights of gravel and sand, respectively, during the rising period of a flood hydrograph [kg];

W_{Tg}, W_{Ts} = total weights of gravel and sand, respectively, during an entire flood hydrograph [kg];

x = streamwise coordinate [m];

α = significance level [–];

κ = von Karman constant [–];

ω = sediment settling velocity [m/s].

References

Adams, J. (1979). Gravel size analysis from photographs. *Journal of the Hydraulics Division, ASCE, 105*(10), 1247-1255.

Bagnold, R. A. (1977). Bed load transport by natural rivers. *Water Resources Research, 13*(2), 303-312.

Bombar, G., Elçi, Ş., Tayfur, G., Güney, M. S.,&Bor, A. (2011). Experimental and numerical investigation of bed-load transport under unsteady flows. *Journal of Hydraulic Engineering, 137*(10), 1276-1282.

Cao, Z. X., Hu, P.,& Pender, G. (2011). Multiple time scales of fluvial processes with bed load sediment and implications for mathematical modelling. *Journal of Hydraulic Engineering, 137*(3), 267-276.

Capart, H., & Young, D. L. (1998). Formation of a jump by the dam-break wave over a granular bed. *Journal of Fluid Mechanics, 372*, 165-187.

Chien, N., & Wan, Z. H. (1999). *Mechanics of sediment transport.* Reston, Virginia, USA: ASCE Press.

Cudden, J. R., & Hoey, T. B. (2003). The causes of bedload pulses in a gravel channel: The implications of bedload grain-size distributions. *Earth Surface Processes and Landforms, 28*(13), 1411-1428.

Einstein, H. A. (1950). The bed-load function for sediment transportation in open channel flows. *Technical Bulletin, No. 1026,* US Department of Agriculture, Washington, D. C.

Engelund, F., & Hansen, E. (1967).*Monograph on sediment transport in alluvial streams.* Copenhagen: Tekniskforlag.

Ferguson, R. I., Prestegaard, K. L., & Ashworth, P. J. (1989). Influence of sand on hydraulics and gravel transport in a braided gravel bed river. *Water Resources Research, 25*(4),

635-643.

Graf, W. H., & Qu, Z. (2004). Flood hydrographs in open channels. *Proceedings of the ICE-Water Management, 157*, 45-52.

Graf, W. H., & Suszka, L. (1985). Unsteady flow and its effects on sediment transport. In *Proceedings of the 21st Congress of IAHR* (pp. 540-544), Melbourne, Australia.

Griffiths, A., &Sutherland, A. S. (1977). Bedload transport by translation waves. *Journal of the Hydraulics Division, ASCE, 103*(HY11), 1279-1291.

Habersack, H. M., Nachtnebel, H. P., & Laronne, J. B. (2001). The continuous measurement of bedload discharge in a large alpine gravel bed river. *Journal of Hydraulic Research, 39*(2), 125-133.

Hassan, M. A., Egozi, R., & Parker, G. (2006). Experiments on the effect of hydrograph characteristics on vertical grain sorting in gravel bed rivers. *Water Resources Research, 42*, W09408.

Hu, P., Cao, Z. X., Pender, G., & Liu, H. H. (2014). Numerical modelling of riverbed grain size stratigraphic evolution. *International Journal of Sediment Research, 29*(3), 329-343.

Kellerhals, R., &Bray, D. I. (1971). Sampling procedures for coarse fluvial sediments. *Journal of the Hydraulics Division, ASCE, 97*(8), 1165-1180.

Kuhnle, R. A. (1992). Bed load transport during rising and falling stages on two small streams. *Earth Surface Processes and Landforms, 17*(2), 191-197.

Kuhnle, R. A. (1993). Fluvial transport of sand and gravel mixtures with bimodal size distributions. *Sedimentary Geology, 85*, 17-24.

Laronne, J. B.,& Reid, I. (1993). Very high rates of bedload sediment transport by ephemeral desert rivers. *Nature, 366*, 148-150.

Lee, K. T., Liu, Y. L., & Cheng, K. H. (2004). Experimental investigation of bedload transport processes under unsteady flow conditions. *Hydrological Processes, 18*(13), 2439-2454.

Li, Z. J., Cao, Z. X., Liu, H. H., & Pender, G. (2016). Graded and uniform bed load sediment transport in a degrading channel. *International Journal of Sediment Research, 31*(4), 376-385.

Lunt, I. A.,& Bridge, J. S. (2007). Formation and preservation of open-framework gravel strata in unidirectional flows. *Sedimentology, 54*, 71-87.

Mao, L. (2012). The effect of hydrographs on bed load transport and bed sediment spatial arrangement. *Journal of Geophysical Research, 117*, F03024.

Meyer-Peter, E.,& Müller, R. (1948). Formulas for bed-load transport. In *Proceedings of the 2nd Congress of IAHR* (pp. 39-64), Stockholm, Sweden.

Parker, G. (1990). Surface-based bedload transport relation for gravel rivers. *Journal of Hydraulic Research, 28*(4), 417-436.

Parker, G., Hassan, M., & Wilcock, P. (2007). Adjustment of the bed surface size distribution of gravel-bed rivers in response to cycled hydrographs. In H. Habersack, H. Piégay, & M. Rinaldi (Eds.), *Gravel bed rivers VI: From process understanding to river restoration* (pp. 241-285). New York: Elsevier.

Phillips, B. C.,& Sutherland, A. J. (1990). Temporal lag effect in bed load sediment transport. *Journal of Hydraulic Research, 28*(1), 5-23.

Qian, H. L., Cao, Z. X., Pender, G., Liu, H. H., & Hu, P. (2015). Well-balanced numerical modelling of non-uniform sediment transport in alluvial rivers. *International Journal of Sediment Research, 30*(2), 117-130.

Reid, I., & Laronne, J. B. (1995). Bed load sediment transport in an ephemeral stream and a comparison with seasonal and perennial counterparts. *Water Resources Research, 31*(3), 773-781.

Song, T., & Graf, W. H. (1997).Experimental study of bedload transport in unsteady open-channel flow. *International Journal of Sediment Research,12*, 63-71.

Wang, L., Cuthbertson, A. J. S., Pender, G., & Cao, Z. X. (2015). Experimental investigations of graded sediment transport under unsteady flow hydrographs. *International Journal of Sediment Research, 30*(4), 306-320.

Wilcock, P. R. (1998). Two-fraction model of initial sediment motion in gravel-bed rivers. *Science, 280*, 410-412.

Wilcock, P. R., & Crowe, J. C. (2003). Surface-based transport model for mixed-size sediment. *Journal of Hydraulic Engineering, 129*(2), 120-128.

Wilcock, P. R., Kenworthy, S. T.,& Crowe, J. C. (2001). Experimental study of the transport of mixed sand and gravel. *Water Resources Research,37*(12), 3349-3358.

Wilcock, P. R., & McArdell, B. W. (1993). Surface-based fractional transport rates: Mobilization thresholds and partial transport of a sand-gravel sediment. *Water Resources Research, 29*(4),1297-1312.

Wong, M., & Parker, G. (2006). One-dimensional modeling of bed evolution in a gravel bed river subject to a cycled flood hydrograph. *Journal of Geophysical Research, 111*, F03018.

Wu, W. M. (2004). Depth-averaged two-dimensional numerical modeling of unsteady flow and nonuniform sediment transport in open channels. *Journal of Hydraulic Engineering, 130*(10), 1013-1024.

Wu, W. M., Wang, S. S.Y., & Jia, Y. F. (2000). Nonuniform sediment transport in alluvial rivers. *Journal of Hydraulic Research,38*(6), 427-434.

Yen, C., & Lee, K. T. (1995). Bed topography and sediment sorting in channel bend with unsteady flow. *Journal of Hydraulic Engineering, 121*(8), 591-599.

Fig. 1. Size distribution of bed sediment

Fig. 2. Flume set-up:(a) perspective view; (b) top view; (c) side view; (d) sediment trap (after Li et al., 2016)

Fig. 3. Designed flow hydrographs at the flume inlet

Fig. 4. Observed stage hydrographs at different cross sections for Run DU2

Fig. 5. Bed elevation for Run DU2: (a) final bed topography (with respect to the initial bed

elevation); (b) cross section averaged initial and final bed elevations; and (c) time variation of cross section averaged bed elevations at $x = 2.0$ m and $x = 6.0$ m

Fig. 6. Bed load transport for Run DU2: (a) total weight; and (b) transport rate averaged in 20-min intervals

Fig. 7. Bed surface composition for Run DU2: (a) the percent of gravel on the initial and final bed surfaces; and (b) time variation of the percentages of gravel (F_g) and sand (F_s) on the bed surface within subsection 2.4< x <3.6 m

Fig. 8. Bed surface composition for Run DS2: (a) the percentage of gravel on the initial and final bed surfaces; and (b) time variation of the percents of gravel (F_g) and sand (F_s) on the bed surface within subsection 2.4< x <3.6 m

Fig. 9. Scaled bed load transport rates for gravel and sand for all the experimental runs

Fig. 10. Variation of the enhancement factor with flow discharge

Fig. 11. Variation of fractional enhancement factor with flow discharge

Fig. 12. Variation of (a) total bed load transport rates (gravel plus sand), (b) scaled gravel transport rates, and (c) scaled sand transport rates for Runs AS1, BS1, CS1, and DS1 with steady inflow

Fig. 13. Variation of (a) total bed load transport rates (gravel plus sand), (b) scaled gravel transport rates, and (c) scaled sand transport rates for Runs AS2, BS2, CS2, and DS2 with steady inflow

Fig. 14. Variation of (a) total bed load transport rates (gravel plus sand), (b) scaled gravel transport rates, and (c) scaled sand transport rates for Runs AU1, BU1, CU1, and DU1 with unsteady inflow

Fig. 15. Variation of (a) total bed load transport rates (gravel plus sand), (b) scaled gravel transport rates, and (c) scaled sand transport rates for Runs AU2, BU2, CU2, and DU2 with unsteady inflow

Fig. 16. Variation of impact factors with flow

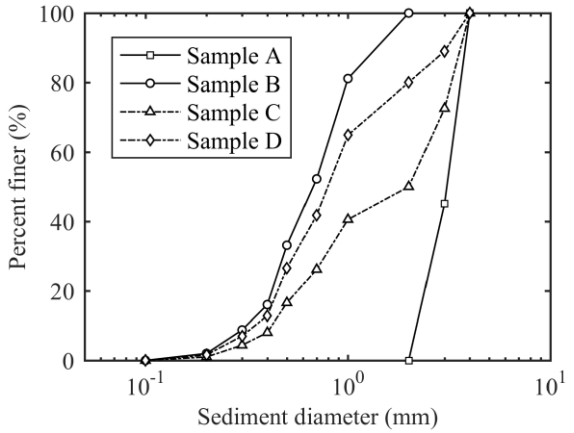

Fig. 1

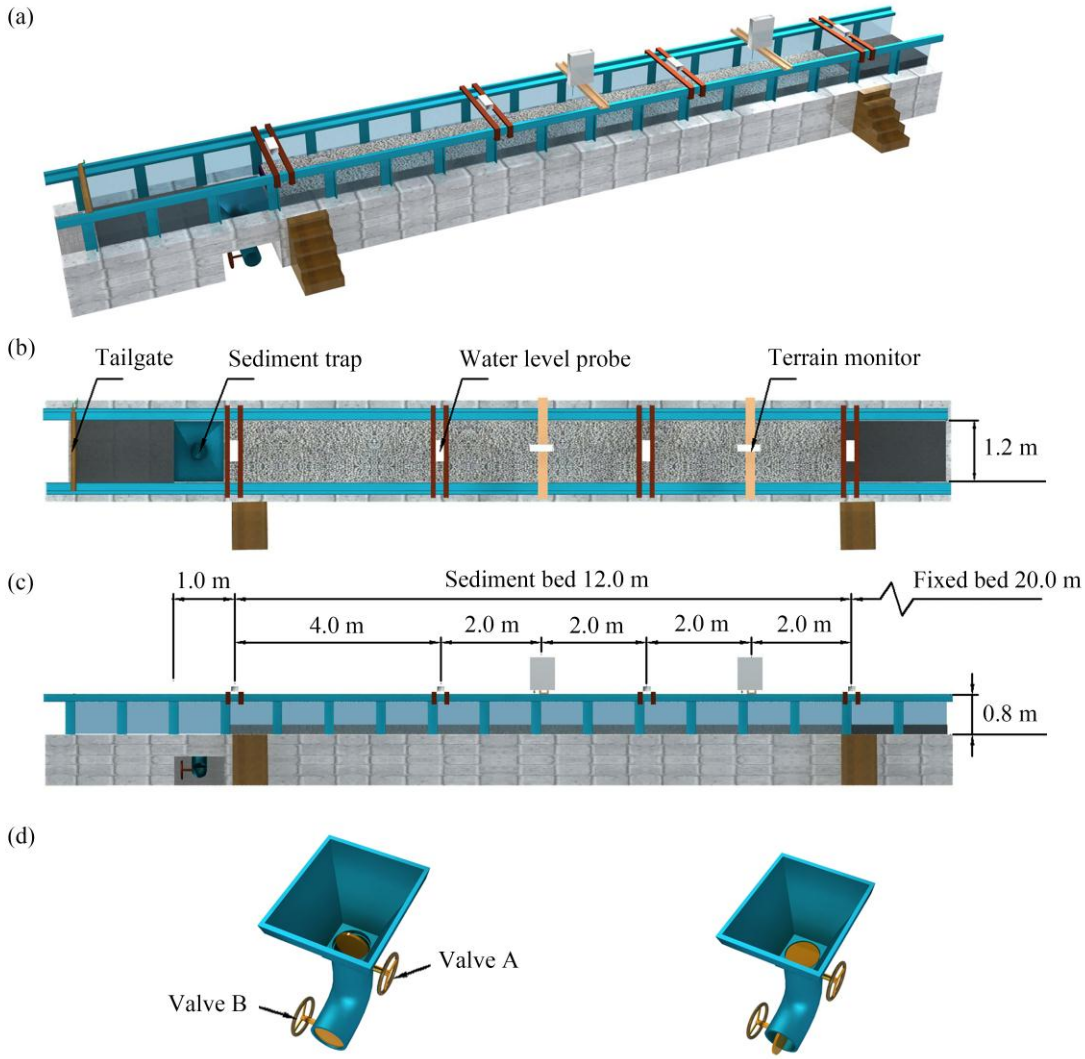
(a)
(b)
Tailgate
Sediment trap
Water level probe
Terrain monitor
1.2 m
(c)
1.0 m
Sediment bed 12.0 m
Fixed bed 20.0 m
4.0 m
2.0 m
2.0 m
2.0 m
2.0 m
0.8 m
(d)
Valve A
Valve B

Fig. 2

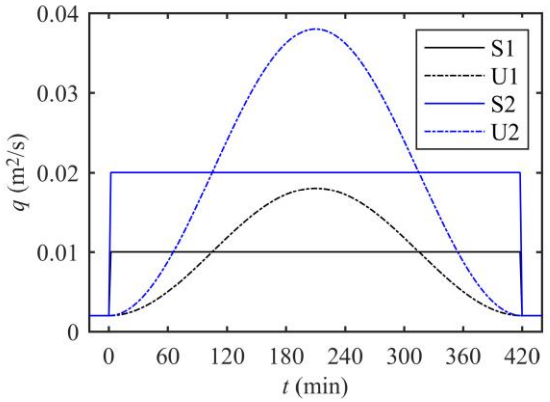
0.04
0.03
0.02
0.01
0
q (m²/s)
S1
U1
S2
U2
0
60
120
180
240
300
360
420
t (min)

Fig. 3

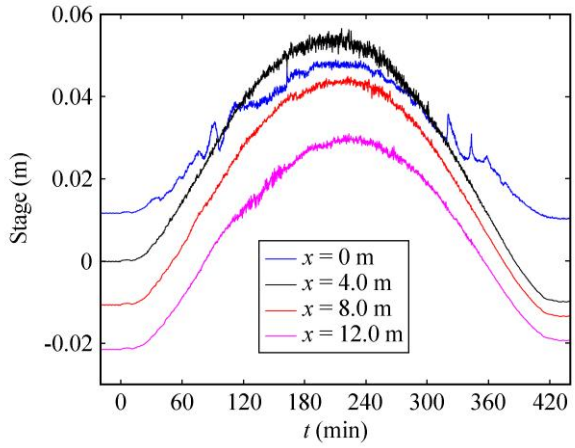

Fig. 4

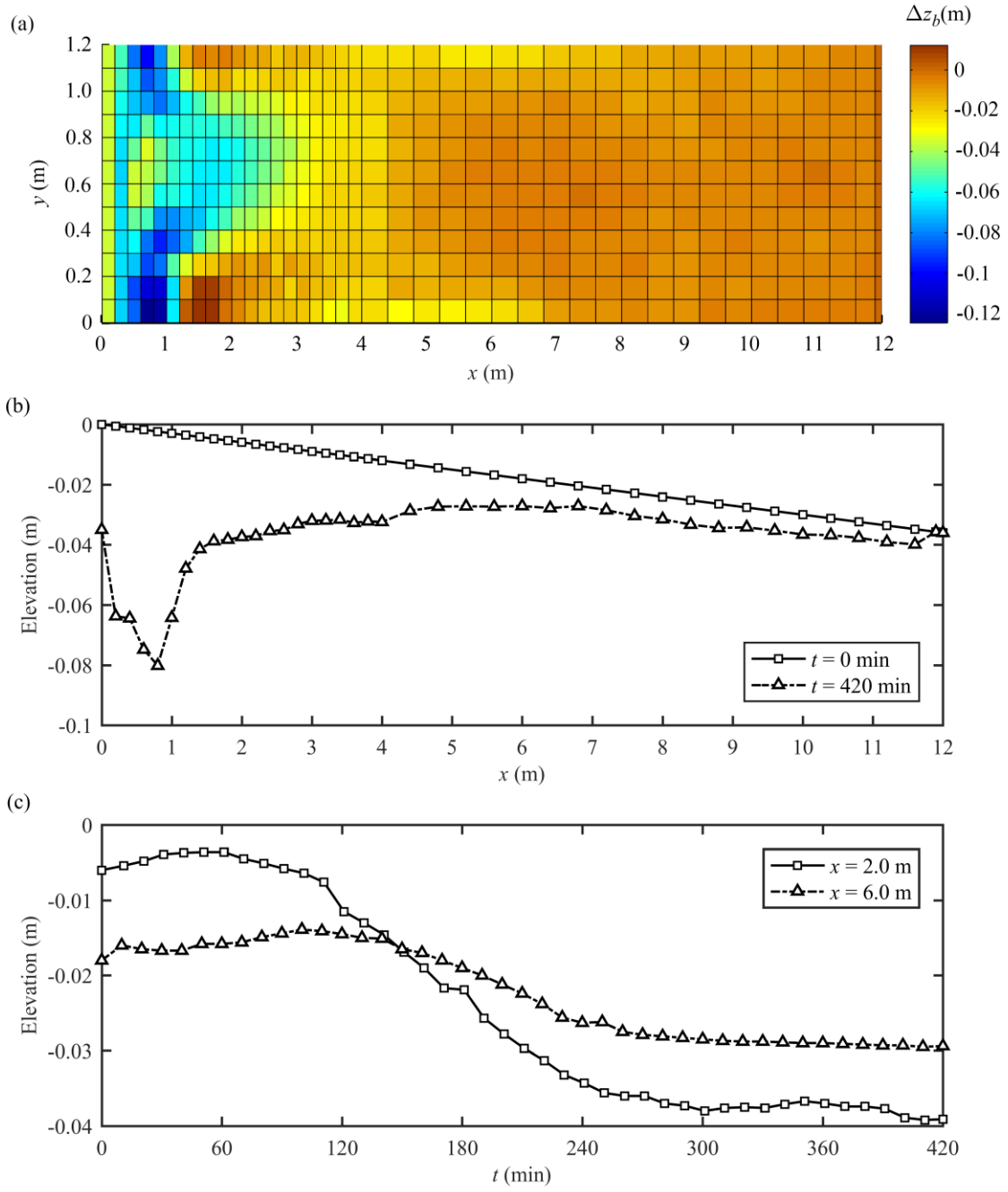

Fig. 5

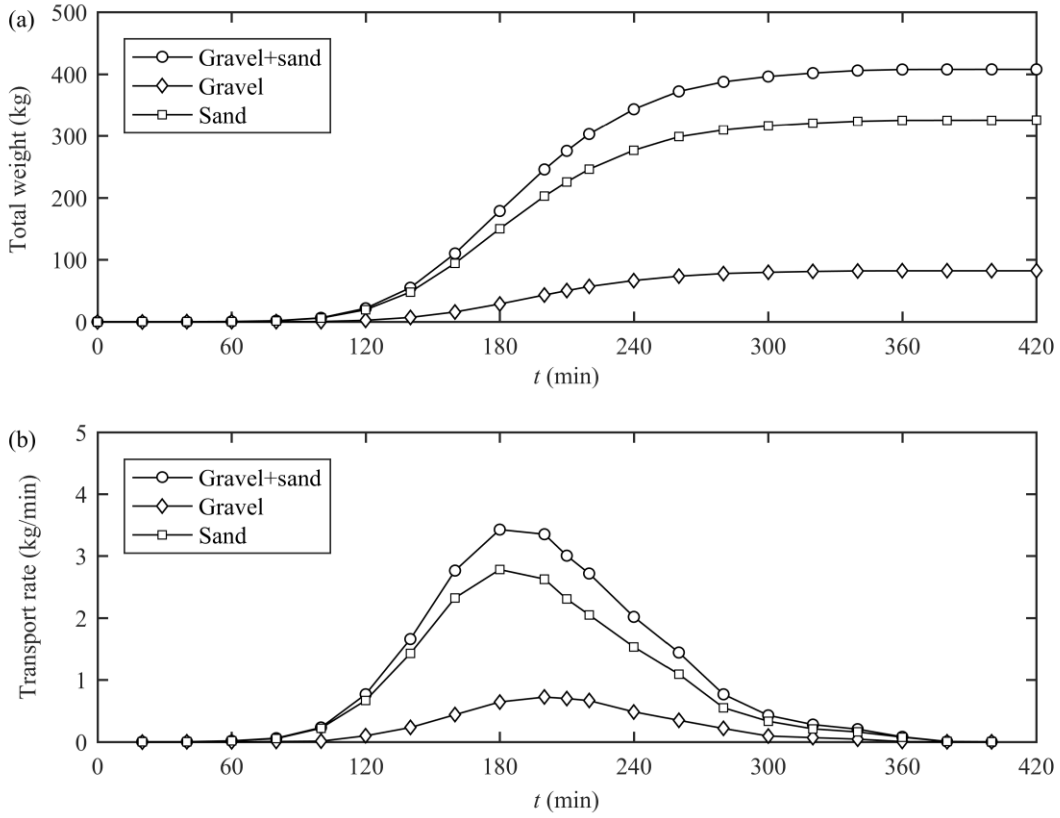

Fig. 6

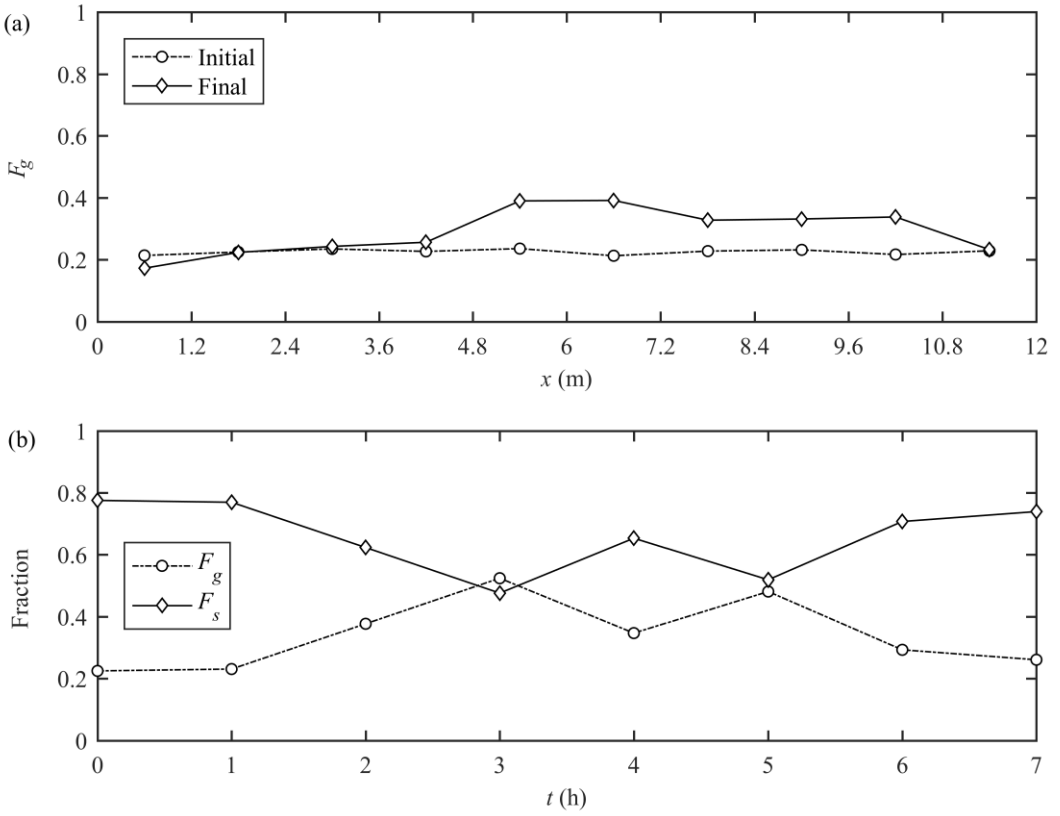

Fig. 7

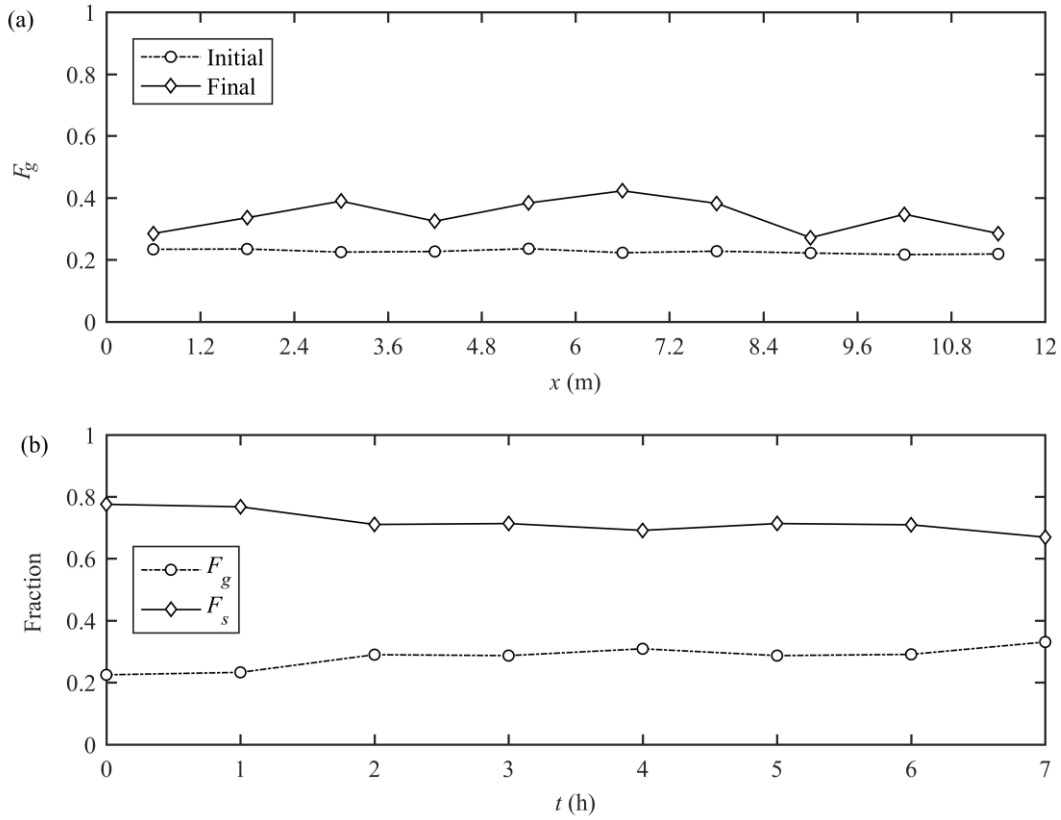

Fig. 8

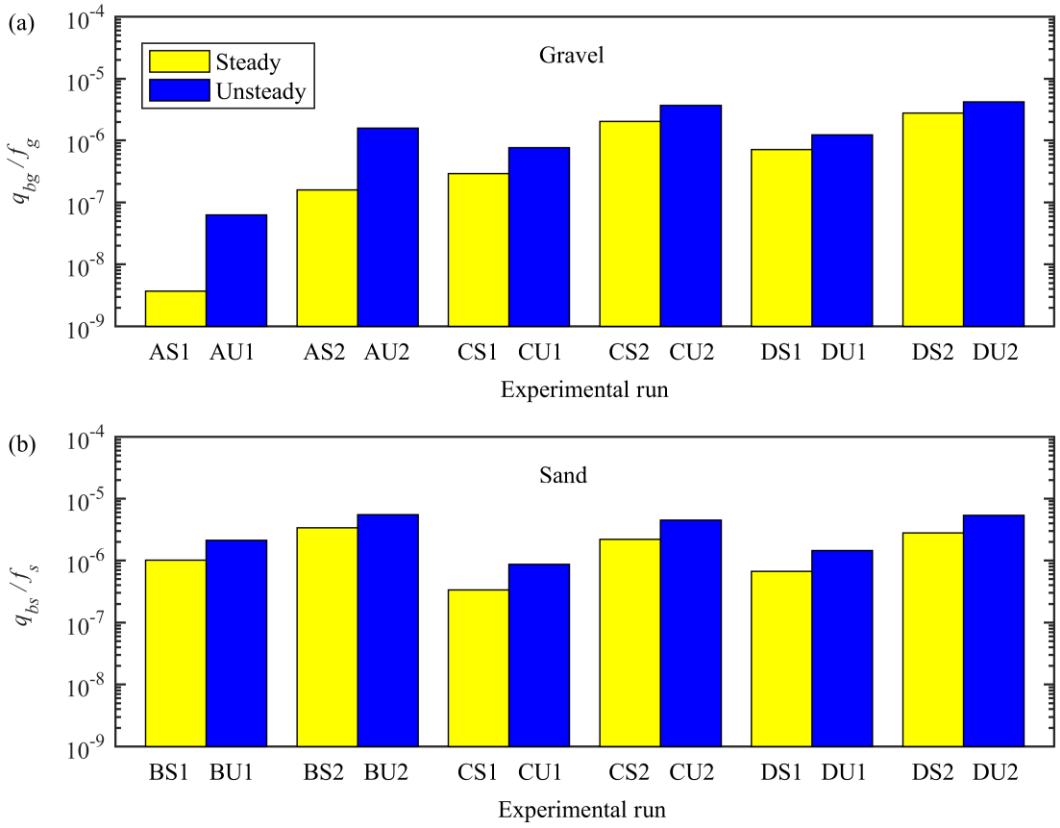

Fig. 9

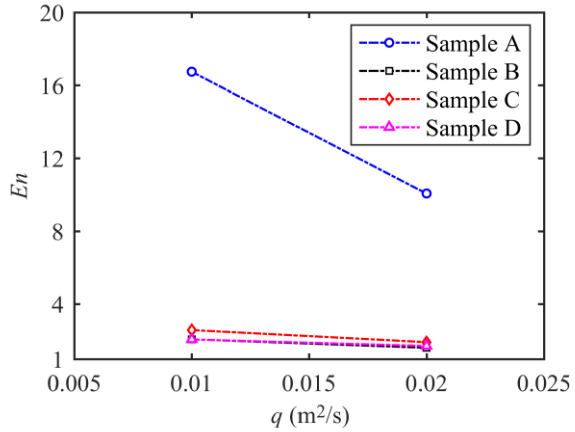

Fig. 10

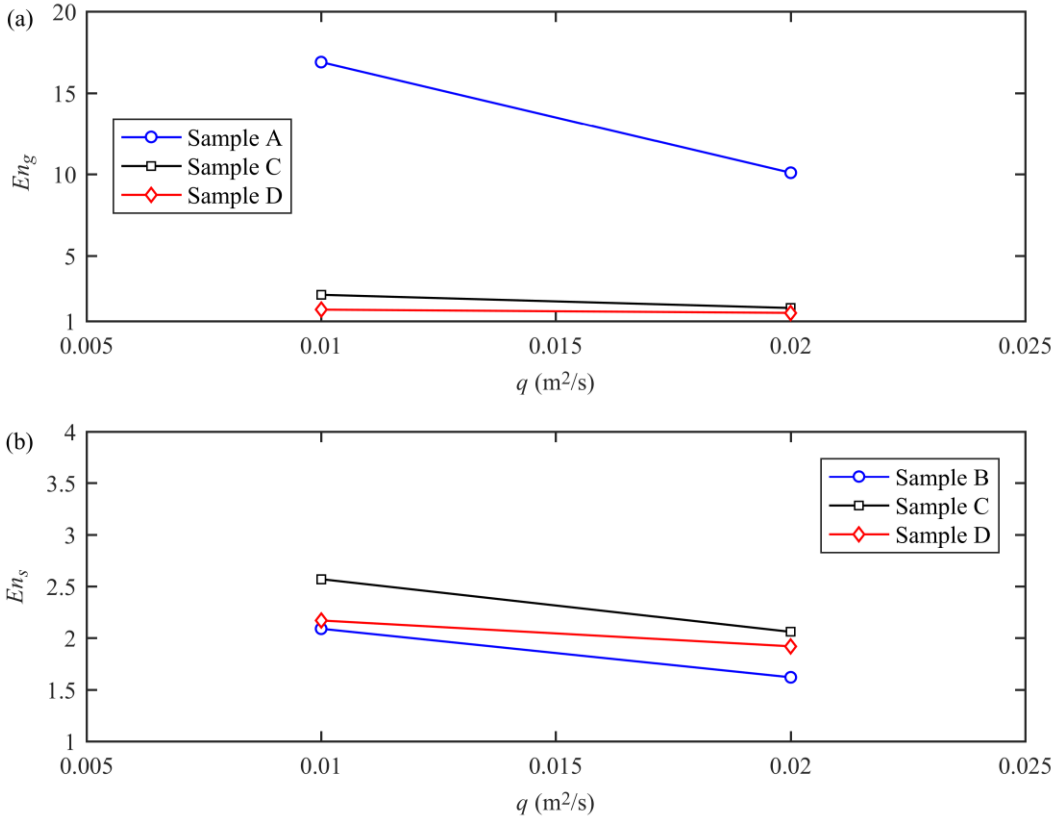

Fig. 11

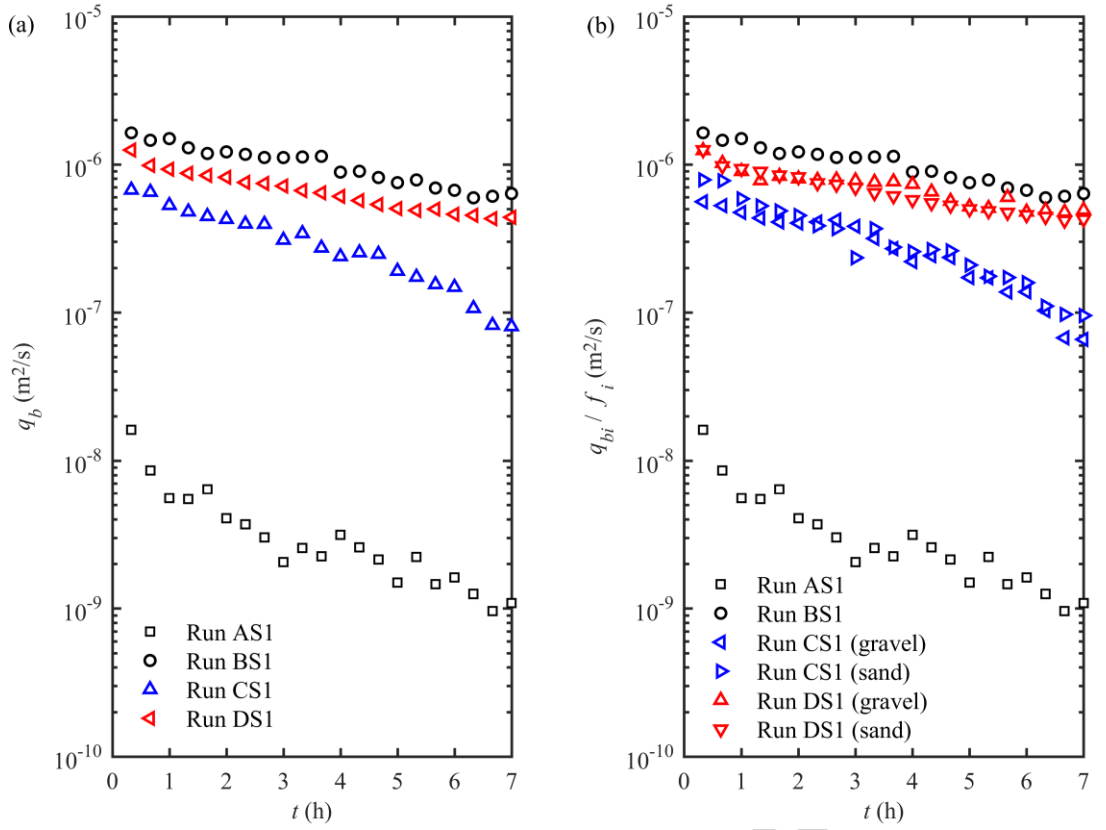

Fig. 12

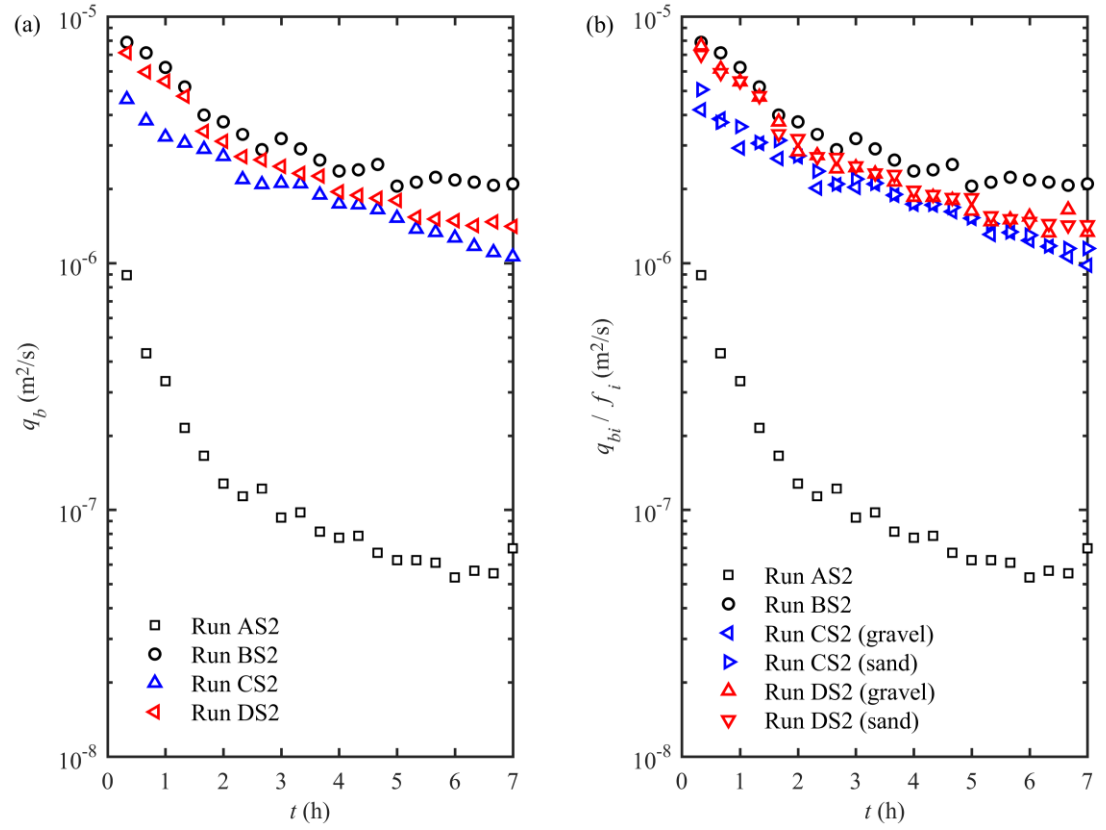

Fig. 13

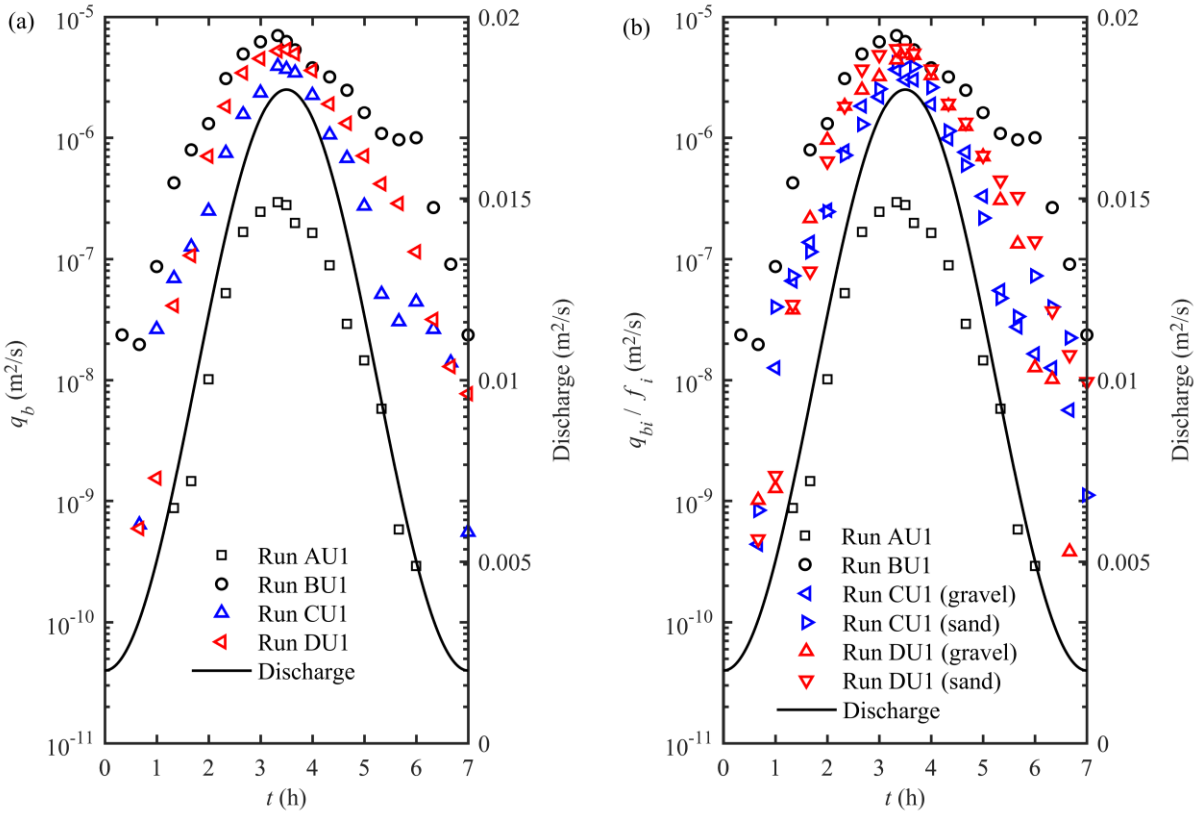

Fig. 14

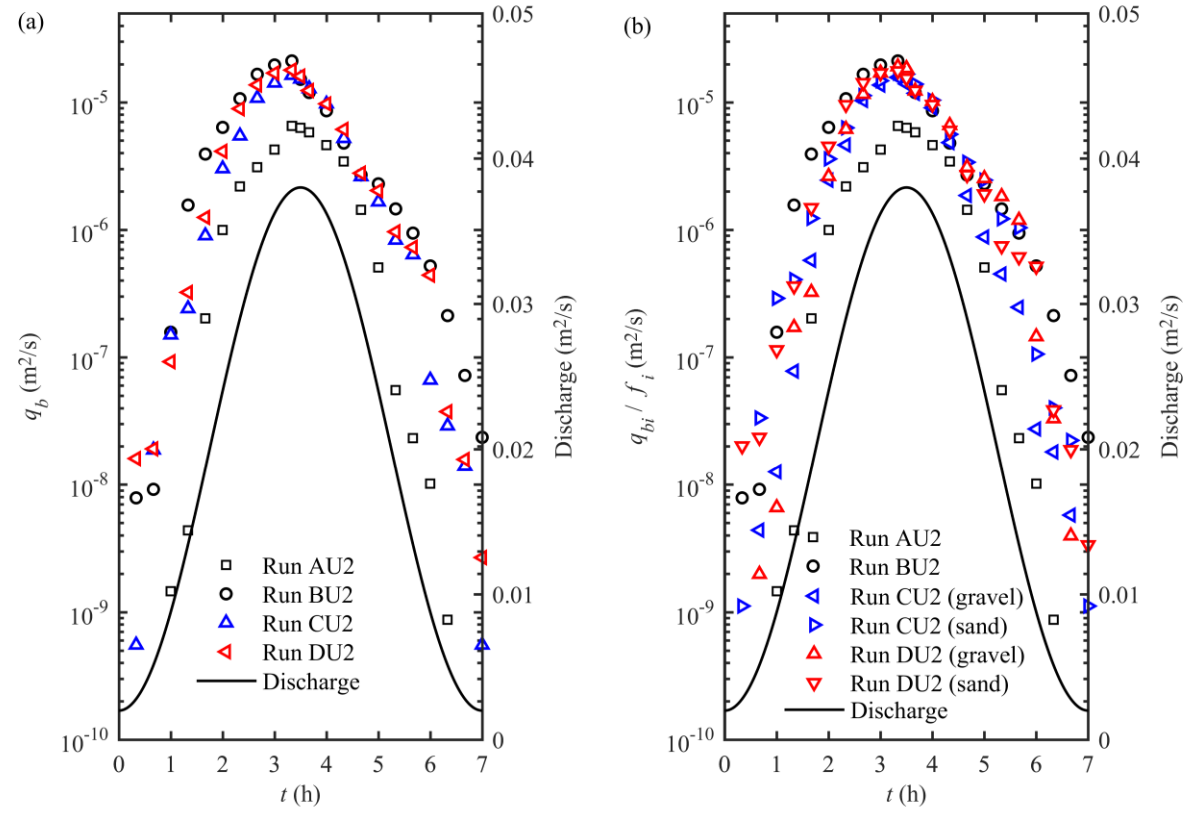

Fig. 15

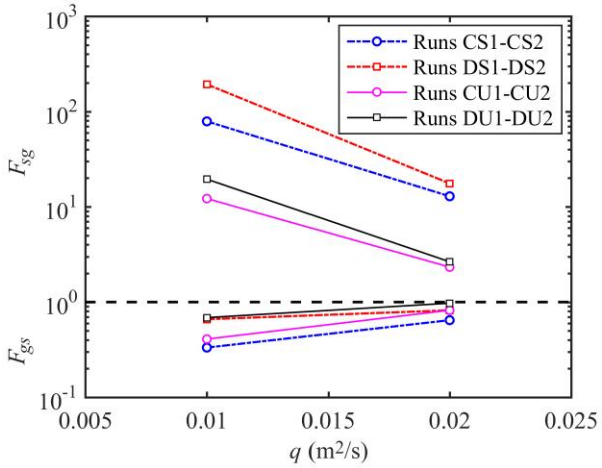

Fig. 16

Table 1. Physical characteristics of bed sediment

Sample	Material	Median size (mm)	Color	Density (kg/m^3)	Porosity
A	100% Gravel	3.1	White	2390	0.426
B	100% Sand	0.67	Yellow	2650	0.412
C	53% Gravel, 47% sand	2.0	/	2513	0.420
D	22% Gravel, 78% sand	0.8	/	2593	0.415

The "/" means the color of bed sediment is hard to define due to the mixing of gravel and sand with different colors.

Table 2. Summary of experiments

Run	Sediment bed	Hydrograph	q (m^2/s)	q_{peak} (m^2/s)	V_{total} (m^3)	SI
AS1	Sample A	S1	0.01	/	302.4	15.1
AS2	Sample A	S2	0.02	/	604.8	13.3
AU1	Sample A	U1	/	0.018	302.4	12.9
AU2	Sample A	U2	/	0.038	604.8	10.2
BS1	Sample B	S1	0.01	/	302.4	6.7
BS2	Sample B	S2	0.02	/	604.8	4.2
BU1	Sample B	U1	/	0.018	302.4	5.3
BU2	Sample B	U2	/	0.038	604.8	4.4
CS1	Sample C	S1	0.01	/	302.4	14.9
CS2	Sample C	S2	0.02	/	604.8	11.0
CU1	Sample C	U1	/	0.018	302.4	10.7
CU2	Sample C	U2	/	0.038	604.8	8.4
DS1	Sample D	S1	0.01	/	302.4	6.3
DS2	Sample D	S2	0.02	/	604.8	5.3
DU1	Sample D	U1	/	0.018	302.4	5.4
DU2	Sample D	U2	/	0.038	604.8	5.0

The "/" indicates no constant or uniform flow discharges for runs with unsteady inflows, and no peak flow discharges for runs with steady inflows.

Table 3. Collected bed load data for the experimental runs

Run	W_{Ti} (kg)		W_{Ri} (kg)		W_{Fi} (kg)		q_{bi} ($\times 10^{-7}$ m^2/s)		q_{bi}/f_i ($\times 10^{-7}$ m^2/s)	
	W_{Tg}	W_{Ts}	W_{Rg}	W_{Rs}	W_{Fg}	W_{Fs}	q_{bg}	q_{bs}	q_{bg}/f_g	q_{bs}/f_s
AS1	0.3	0.0	/	/	/	/	0.04	0.00	0.04	0.00
AS2	11.4	0.0	/	/	/	/	1.58	0.00	1.58	0.00
AU1	4.5	0.0	3.1	0.0	1.4	0.0	0.63	0.00	0.63	0.00
AU2	114.8	0.0	70.2	0.0	44.6	0.0	15.90	0.00	15.90	0.00
BS1	0.0	81.1	/	/	/	/	0.00	10.10	0.00	10.10
BS2	0.0	271.6	/	/	/	/	0.00	33.90	0.00	33.90
BU1	0.0	168.9	0.0	103.3	0.0	65.6	0.00	21.10	0.00	21.10
BU2	0.0	440.2	0.0	335.1	0.0	105.1	0.00	54.90	0.00	54.90
CS1	11.2	12.6	/	/	/	/	1.55	1.58	2.92	3.36
CS2	78.7	82.8	/	/	/	/	10.80	10.30	20.40	21.90
CU1	29.3	32.5	19.1	20.4	10.2	12.1	4.05	4.06	7.64	8.64
CU2	141.7	169.6	99.4	113.6	42.4	56.0	19.60	21.20	37.00	45.10
DS1	11.3	41.7	/	/	/	/	1.57	5.20	7.14	6.67
DS2	44.2	174.2	/	/	/	/	6.12	21.70	27.80	27.80
DU1	19.4	90.7	11.9	57.5	7.5	33.2	2.68	11.30	12.20	14.50
DU2	74.2	301.0	50.2	216.6	24.0	84.5	9.26	41.70	42.10	53.50

The "/" means no collected data for rising or falling period when it comes to runs with steady inflows, where flow hydrographs are always constant and uniform without rising or falling process.

Table 4. Summary of *t*-values

Runs	*t*-value	Remark	Runs	*t*-value	Remark
AS1 vs. CS1	8.130	Fig. 12b (gravel)	AS2 vs. CS2	10.379	Fig. 13b (gravel)
AS1 vs. DS1	13.072		AS2 vs. DS2	7.167	
CS1 vs. DS1	15.726		CS2 vs. DS2	2.008	
BS1 vs. CS1	15.443	Fig. 12c (sand)	BS2 vs. CS2	6.434	Fig. 13c (sand)
BS1 vs. DS1	11.595		BS2 vs. DS2	10.719	
CS1 vs. DS1	11.462		CS2 vs. DS2	3.316	
AU1 vs. CU1	3.413	Fig. 14b (gravel)	AU2 vs. CU2	3.246	Fig. 15b (gravel)
AU1 vs. DU1	3.744		AU2 vs. DU2	3.537	
CU1 vs. DU1	3.927		CU2 vs. DU2	3.714	
BU1 vs. CU1	5.102	Fig. 14c (sand)	BU2 vs. CU2	1.861	Fig. 15c (sand)
BU1 vs. DU1	5.837		BU2 vs. DU2	2.365	
CU1 vs. DU1	3.459		CU2 vs. DU2	0.931	